Archives of Environmental Contamination and Toxicology (2024) 86:393–409
https://doi.org/10.1007/s00244-024-01070-0

Insight Study of Trace Elements in $PM_{2.5}$ During Nine Years in Delhi, India: Seasonal Variation, Source Apportionment, and Health Risks Assessment

Sakshi Gupta[1,2] · Sudhir Kumar Sharma[1,2] · Preeti Tiwari[1,2] · Narayanasamy Vijayan[1,2]

Received: 29 January 2024 / Accepted: 15 May 2024 / Published online: 28 May 2024

Abstract

This study investigated the concentrations, seasonal variations, sources, and human health risks associated with exposure to heavy elements (As, Al, Pb, Cr, Mn, Cu, Zn, and Ni) of $PM_{2.5}$ at an urban location of Delhi (28° 38′ N, 77° 10′ E; 218 m amsl), India, from January 2013 to December 2021. The average mass concentration of $PM_{2.5}$ throughout the study period was estimated as 127 ± 77 μg m^{-3}, which is exceeding the National Ambient Air Quality Standards (NAAQS) limit (annual: 40 μg m^{-3}; 24 h: 60 μg m^{-3}). The seasonal mass concentrations of $PM_{2.5}$ exhibited at the order of post-monsoon (192 ± 110 μgm^{-3}) > winter (158 ± 70 μgm^{-3}) > summer (92 ± 44 μgm^{-3}) and > monsoon (67 ± 32 μgm^{-3}). The heavy elements, Al (1.19 μg m^{-3}), Zn (0.49 μg m^{-3}), Pb (0.43 μg m^{-3}), Cr (0.21 μg m^{-3}), Cu (0.21 μg m^{-3}), Mn (0.07 μg m^{-3}), and Ni (0.14 μg m^{-3}) exhibited varying concentrations in $PM_{2.5}$, with the highest levels observed in the post-monsoon season, followed by winter, summer, and monsoon seasons. Six primary sources throughout the study period, contributing to $PM_{2.5}$ were identified by positive matrix factorization (PMF), such as dust (paved/crustal/soil dust: 29.9%), vehicular emissions (17.2%), biomass burning (15.4%), combustion (14%), industrial emissions (14.2%), and Br-rich sources (9.2%). Health risk assessments, including hazard quotient (HQ), hazard index (HI), and carcinogenic risk (CR), were computed based on heavy elements concentrations in $PM_{2.5}$. Elevated HQ values for Cr and Mn linked with adverse health impacts in both adults and children. High carcinogenic risk values were observed for Cr in both adults and children during the winter and post-monsoon seasons, as well as in adults during the summer and monsoon seasons. The combined HI value exceeding one suggests appreciable non-carcinogenic risks associated with the examined elements. The findings of this study provide valuable insights into the behaviour and risk mitigation of heavy elements in $PM_{2.5}$, contributing to the understanding of air quality and public health in the urban environment of Delhi.

Particulate matter (PM) emerges as a crucial atmospheric pollutant, exerting significant impact over the air quality in India and globally (Singh 2019). Its harmful potential and alarming concentrations make it a leading concern for environmental well-being (WHO 2016). The urban region of Delhi, India, stands at the crossroads with rapidly increasing industrialization, population expansion, and urbanization, resulting in significant challenges related to air quality (Jerret 2015; Leliveld et al. 2015; Jain et al. 2020a; Zhu et al. 2020). Among the various pollutants of concern, PM with a diameter of 2.5 μm or smaller ($PM_{2.5}$) has emerged as a critical focus due to its harmful impact on both air quality and public health (Dockery et al. 1993; Pope and Dockery 2009; Joshi et al. 2022; Colonna et al. 2022; Zhang et al. 2022). The adverse effects of prolonged exposure to elevated $PM_{2.5}$ levels are associated with respiratory and cardiovascular ailments, posing a substantial risk to the well-being of the city's inhabitants (Joshi et al. 2022; Colonna et al. 2022; Jin et al. 2022). In recent years, the scientific community and public authorities worldwide have increasingly expressed significant concern about the effects of PM on both climate and human health (IPCC 2013).

This study begins on a comprehensive investigation aimed at unravelling the complexities of $PM_{2.5}$ pollutions in Delhi. The focus extends beyond merely quantifying overall $PM_{2.5}$ concentrations, studying the detailed analysis

✉ Sudhir Kumar Sharma
sudhir@nplindia.org; sudhircsir@gmail.com

[1] CSIR-National Physical Laboratory, Dr. K. S. Krishnan Road, New Delhi 110012, India

[2] Academy of Scientific and Innovative Research (AcSIR), Ghaziabad 201002, India

of elemental compositions present in these fine particles (Chen et al. 2020; Verma et al. 2023). The introduction of these elements into the atmosphere has the potential to pose a significant threat to terrestrial and aquatic ecosystems through dry/wet deposition, subsequently endangering human health as a result of physico-chemical transfer and bioaccumulation within food chains (Storelli 2008; Harmens et al. 2010). Certain toxic trace elements such as As, Pb, and Cr are commonly recognized as human carcinogens, even when present in minute quantities (Micheline et al. 2019). Moreover, the disproportionate build-up of certain biologically essential elements like Cu, Fe, Zn, etc. has the potential to trigger inflammatory cascades in tissues (Saffari et al. 2014). Additionally, this accumulation can trigger biochemical synthesis pathways by catalysing the production of reactive oxygen species (ROS) (Saffari et al. 2014; Lopez Cruz et al. 2016). It is important to highlight that, although a moderate enrichment of these elements can be advantageous for human health and plant growth, excessive levels may result in adverse effects. (Oldani et al. 2017). Several studies identified various elements present in $PM_{2.5}$ originated from number of sources, including vehicular emissions, industrial activities, and natural sources, each contributing to the complex composition of urban air pollution (Chakraborty and Gupta 2010; Behera et al. 2011; Sharma et al. 2016a, 2016b; Sharma and Mandal. 2017; Jain et al. 2018, 2019, 2020a, 2020b; Murari et al. 2020).

In addition to elucidating the elemental composition, this research employs advanced source apportionment techniques, i.e. positive matrix factorization (PMF) model to discern the origins of $PM_{2.5}$ pollutants. Identifying and understanding the primary contributors to air pollution are pivotal steps towards formulating targeted and effective strategies for pollution reduction (Rai et al. 2020a, b; Sharma and Mandal 2023). Through this approach, we aim to provide policymakers, environmental agencies, and the public with insights into the specific sources that warrant immediate attention and intervention. Crucially, the study goes beyond the realm of concentration and source identification to conduct a rigorous human health risk assessment associated with the elemental components of $PM_{2.5}$. This multifaceted analysis considers potential short-term and long-term health impacts, offering a comprehensive understanding of the risks posed by specific elements within the $PM_{2.5}$. The metallic constituents found in PM, particularly the fine fraction containing elements like Fe, Ni, Cu, As, Pb, Mn, and Cr are evidently major contributors to the development of both pulmonary and cardiovascular diseases (Kelly and Fussell 2012; Joshi et al. 2022).

As Delhi deal with both rapid urban development and deteriorating air quality, the results of this research aim to provide insights for evidence-based policies and interventions. By unravelling the complexities of $PM_{2.5}$ pollutions in the city, we aspire to contribute valuable knowledge that can guide mitigation strategies, enhance air quality management, and ultimately safeguard the health and resilience of Delhi's diverse population.

Methodology

$PM_{2.5}$ Sampling and Analysis

756 $PM_{2.5}$ samples (2 samples/week) were collected at the monitoring site of CSIR-National Physical Laboratory, New Delhi (28° 38′ N, 77° 10′ E; 218 m amsl), India (Fig. 1), from January 2013 to December 2021 except Covid-19 lockdown period (lockdown periods: 25 March, 2020–31 May, 2020; 5 April, 2021–15 June 2021). $PM_{2.5}$ samples were collected on pre-combusted (550 °C) Pallflex quartz fibre filters using a $PM_{2.5}$ sampler (APM 550; Envirotech, India). The sampler was positioned at a height of 10 m above the ground (AGL), and it maintained an average flow rate of 1 m^3 h^{-1} with an accuracy of ± 2%. Following the guidelines set by the Central Pollution Control Board (CPCB), 24-h sampling was conducted during the entire study period (2013–2021) (Jain et al. 2020a, b). Preceding and succeeding the sampling process, filters were desiccated (dried), and a microbalance with a resolution of ± 0.01 mg was employed to determine the initial and final weights. The gravimetric method was utilized to compute the mass concentration of $PM_{2.5}$. The concentration of $PM_{2.5}$ (μg m^{-3}) was determined by subtracting the initial weight from the final weight of the QM-A filters, which were measured using a microbalance. This difference was then divided by the total volume of air sampled during the collection process. Following sample collection, the filters were stored under dry conditions in a deep-freezer at − 20 °C before undergoing analysis. The sampling location exemplifies a standard urban setting, bordered by intense roadside traffic and agricultural fields extending in the south-west direction.

The elemental analysis of $PM_{2.5}$ was conducted using a wavelength-dispersive X-ray fluorescence spectrometer (WD-XRF; ZSX Primus, Rigaku, Japan), operating under standard conditions, including vacuum, 36 °C temperature, and a 2.4 kW tube rating. Calibration was regularly performed with micro-matter thin-film standards as per recommended standard procedure (Watson et al. 1999). The $PM_{2.5}$ samples revealed the presence of elements like Al, Fe, Zn, Mn, Ti, Cu, Cr, Ni, Cl, P, S, K, Mo, Na, Mg, Ca, Pb, As, and Br, with occasional non-detection of Mo and Ni. For quality check and quality assurance (QA/QC), the measurements of field blank filters were also conducted, which were subsequently utilized for intensity correction (as well as field blank correction) of the $PM_{2.5}$ exposed filters. Through triplicate ($n = 3$) analysis of the sample filters, the

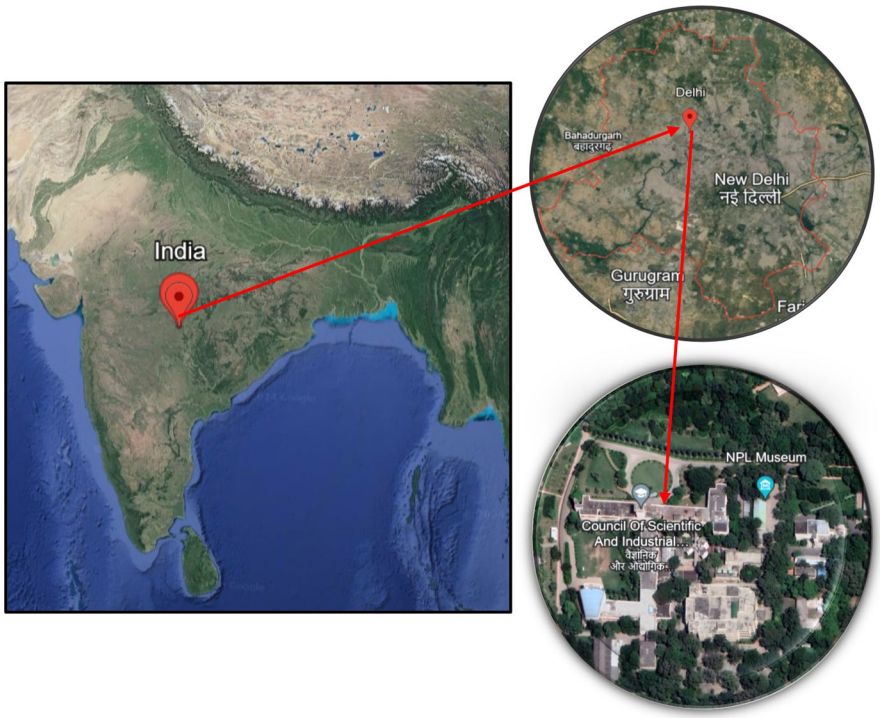

Fig. 1 Map of the study site (*Source*: Google Earth)

analytical error or repeatability measurement was estimated to be approximately 5–10% (Table S1; in supplementary information). The method detection limit (MDL) for the observed elements was estimated as three times of average standard deviation (SD) of 10 replicate filed blank samples filters (Jain et al. 2017). The estimated values of MDL (μg m^{-3}) and % repeatability errors are given in Table S1 (in supplementary information). Elemental concentrations were analysed using SPSS software (IBM, version 26.0), adhering to standard statistical procedures, as outlined in our previous publications for a comprehensive insight into the measurement methodology (Jain et al. 2020a; Sharma et al. 2021).

Air Mass Backward Trajectories, Potential Source Contribution Function (PSCF), and Conditional Bivariate Probability Function (CBPF)

Air mass backward trajectory analysis utilized Air Resources Laboratory (ARL) datasets Hybrid Single-Particle Lagrangian Integrated Trajectory model (HYSPLIT), tracing $PM_{2.5}$ pathways from the receptor site at 500 m AGL. TrajStat software generated and analysed 120-h trajectories (Rai et al. 2020a, b; Jain et al. 2020a, b; Choudhary et al. 2022). The backward trajectory analysis generates extensive sets of trajectories, delineating the spatial extent of air parcels reaching a designated receptor site. These trajectories elucidate the airflow patterns directing air masses towards the study area, Delhi, originating from diverse regions across the Indian subcontinent, at three distinct elevations (500 m, 1000 m, and 1500 m AGL). The CBPF approach in R-studio, with meteorological data from automated weather station (AWS), represented source regions in polar coordinates. Polar plots, using Open-air package, focused on $PM_{2.5}$ concentrations and 75th percentiles for the study (Uria-Tellaetxe and Carslaw 2014; Banoo et al. 2024).

Positive Matrix Factorization (PMF)

Utilizing the USEPA PMF 5.0 involves decomposing a speciated data matrix (X) into factor contribution (C) and profile (P) matrices, along with a residual matrix (e). This multivariate factor analysis model aims to elucidate the chemical mass balance by examining the relationship between computed concentrations and source profiles, providing insights into the contributions of various sources to the overall data (Paatero et al. 1997; Paatero and Tapper 1994) (Eq. 1).

$$X = C \times P + \mathrm{e} \tag{1}$$

The standard equation-based uncertainty (U) is derived through an Eq. 2 that incorporates the error fraction (ef), concentration (C), and the method detection limit (MDL) of the species (Gianini et al. 2012). The signal-to-noise ratio (S/N) for each species serves as an indicator of measurement heterogeneity, reflecting the absolute measurement or the measurement within the noise (Brown et al. 2015).

$$U = \sqrt{(\text{ef} \times \text{C})^2 + (0.5 \times \text{MDL})^2} \quad (2)$$

$$U = \frac{5}{6} \times \text{MDL}, C < \text{MDL}$$

The PMF model's primary output, detailing contribution and profile, is derived from the initial base run, with the Q value serving as a key indicator of goodness of fit. Q-robust, excluding values with scaled residuals exceeding 4, is compared to Q-true, providing insights into the global minimum. Analysis of Q-robust strength and random seeds aids in this determination. Species with significant residuals indicate poor fitting, with a preferred range of −3 to +3 indicative of a normal distribution. For error estimation, DISP, BS, and BS-DISP methods are utilized. DISP considers rotational discrepancies and is influenced by user-specified data uncertainty, while the BS interval remains unaffected by such specifications. The BS-DISP method accommodates both rotational uncertainties and random errors, despite its susceptibility to mis-specifying data uncertainty (Gupta et al. 2012; Singhal et al. 2017; Jain et al. 2019, 2020a; Li et al. 2020; Rai et al. 2020a, b; Rai et al. 2021; Choudhary et al. 2023; Banoo et al. 2024).

In this study, we utilized PMF version 5.0. The PMF model analyses both input and equation-based uncertainty data files to gain insights into the sources and their respective percentage profiles. In the present scenario, we performed annual (pooled for 2013–2021 datasets) as well as seasonal (winter, summer, monsoon, and post-monsoon) source apportionment by applying PMF model. The seasonal PMF analysis was not derived from or influenced by the annual PMF observations. This approach ensured that each analysis was treated as distinct and allowed for a more focused examination of the seasonal variations without the potential biases introduced by the annual data. By conducting separate analyses, we were able to better understand the specific dynamics and patterns present within each seasonal dataset (ref. to supplementary information text S1). The input data file includes elemental composition of $PM_{2.5}$ (i.e. Na, K, Mg, Ca, Al, S, Ti, Mn, Fe, Cu, Zn, As, Br, Pb, Cr, Cl, P, and Mo). Equation-based uncertainty was computed using Eq. (2), which corresponds to the input speciated data. The identification of sources at study sites involved integrating model data (S/N, R^2, time series) with the base model and error estimation. In the case of the BS method, 100 runs were conducted, and the results are deemed valid as all factors exhibited a mapping accuracy above 75% in all the cases except post-monsoon due to the significant environmental changes, such as altered vegetation and water level. Also, certain natural processes occur during post-monsoon that may introduced variability in BS. The DISP analysis provided additional confirmation of the solution's stability, with the observed decrease in the Q value being less than 0.1%, and no factor swap was noted. In the BS-DISP analysis, the solution was deemed reliable, as the observed decline in the Q value was below 0.5%. Furthermore, both the BS and BS-DISP results showed no signs of asymmetry or rotational ambiguity for all factors. The further detailed information about the S/N ratio, R^2 and model inputs is given in supplementary information (Tables S2, S3). The potential number of factors is determined based on the $Q_{true}/Q_{expected}$ value (refer to Fig. S9), where a value closer to 1 indicates a more reliable number of factors.

Health Risk Assessment (HRA) of Trace/Heavy Elements of $PM_{2.5}$

Being a typical urban area, Delhi accommodates a significant population and grapples with poor air quality (Verma et al. 2023). Consequently, residents in Delhi could face substantial exposure risks associated with trace elements (Prakash et al. 2018). In this study, we assessed the carcinogenic and non-carcinogenic risks linked to trace elements in $PM_{2.5}$, employing statistical thresholds outlined by the International Agency for Research on Cancer (IARC). Following the IARC criteria, elements such as As, Ni, Cr, and Pb were identified as having carcinogenic potential for humans. HRA computation was performed utilizing criteria recommended by the USEPA and data sourced from the Integrated Risk Information System (IRIS) for assessing the carcinogenic and non-carcinogenic risks associated with Al, Zn, Mn, Cr, Cu, Ni, As, and Pb through inhalation exposure to $PM_{2.5}$. The exposure concentration (μg m^{-3}) (EC), hazard quotient (HQ), and carcinogenic risk (CR) were determined by applying Eqs. (3–5) (USEPA 2011).

$$\text{EC} = \frac{C \times \text{ET} \times \text{EF} \times \text{ED} \times \text{IR}}{\text{AT} \times \text{BW}} \quad (3)$$

In the context of non-carcinogenic risk assessment, the hazard quotient (HQ) is determined using the following parameters: C represents the element's composition in ambient air (μg m^{-3}), ET stands for exposure time (12 h per day) (h/day), EF represents exposure frequency (days/year) (350 days/year), ED represents exposure duration (years) (6 for children and 24 for adults), IR denotes the rate of air inhalation, specifically 10 m^3 per day for children and 20 m^3 per day for adults, AT represents the average time (days/year) (365*ED), and BW signifies body weight, which is 15 kg for children and 70 kg for adults.

$$\text{HQ} = \frac{\text{EC}}{\left(Rf_c \times \text{CF}\right)} \quad (4)$$

In this context, where Rf_c represents the reference concentration in mg m^{-3} and CF is the conversion factor with a

value of 1000 μg mg^{-1}. An HQ value less than or equal to 1 implies a safe condition with no health hazard, while an HQ greater than or equal to 1 suggests the possibility of a health hazard and potential adverse health effects.

For carcinogenic risk assessment,

$$CR = IUR \times EC \quad (5)$$

In the context of inhalation unit risk (IUR), if the calculated carcinogenic risk (CR) exceeds 10^{-4}, it indicates a high risk of cancer. A CR value ranging between 10^{-6} and 10^{-4} is deemed within acceptable limits, while a CR value below 10^{-6} is considered to have mild health effects (Zheng et al. 2010; Prakash et al. 2018; Ma et al. 2018; Zhang et al. 2018; Wang et al. 2022; Gupta et al. 2023). The Rf_c and IUR values for their respective heavy elements are given in Table S4 (in supplementary information).

Results and Discussion

$PM_{2.5}$ Concentrations and Elemental Compositions

The annual average mass concentrations (± SD) of $PM_{2.5}$ were reported as follows: 136 ± 91 μg m^{-3}, 113 ± 96 μg m^{-3}, 123 ± 65 μg m^{-3}, 138 ± 58 μg m^{-3}, 143 ± 70 μg m^{-3}, 124 ± 70 μg m^{-3}, 129 ± 96 μg m^{-3}, 116 ± 68 μg m^{-3}, and 109 ± 53 μg m^{-3} for the years 2013, 2014, 2015, 2016, 2017, 2018, 2019, 2020, and 2021, respectively, whereas the annual median mass concentrations of $PM_{2.5}$ were recorded as 105.4 μg m^{-3} (2013), 77.7 μg m^{-3} (2014), 103.8 μg m^{-3} (2015), 123.9 μg m^{-3} (2016), 120.0 μg m^{-3} (2017), 71.5 μg m^{-3} (2018), 97.5 μg m^{-3} (2019), 105.7 μg m^{-3} (2020), and 70.3 μg m^{-3} (2021) during the sampling period. The average $PM_{2.5}$ concentrations in 2020 and 2021 were relatively low, a consequence of decreased activities during the Covid-19 lockdown period as opposed to the pre-Covid-19 era with restricted activities (Sharma and Mandal 2023). The overall average concentration of $PM_{2.5}$ for the years 2013–2021 was found to be 126 ± 77 μg m^{-3}, i.e. ~ 3 times higher than the National Ambient Air Quality Standards (NAAQS) limit for annual (40 μg m^{-3}). Similar concentration was reported by previous researchers in Delhi and Agra (Jain et al. 2021; Sharma et al. 2022; Sah et al. 2022) over the northern IGP regions of India. Throughout the entire sampling duration, WD-XRF identified 19 elements (Na, K, Mg, Ca, Al, S, Ti, Mn, Fe, Cu, Zn, As, Br, Pb, Cr, Cl, P, Mo, and Ni) consistently in all $PM_{2.5}$ samples (Table 1). The supplementary Figures S2-3 represented the temporal variation of major elements (Al, Fe, Mn, K, Mg, and Ca) and trace elements (Cu, Zn, Cr, Br, Pb, and Mo) present in $PM_{2.5}$ at Delhi from 2013 to 2021. The maximum overall annual average concentrations (± SD) including median concentrations were reported for Cl (average: 3.44 ± 2.68 μg m^{-3}; median: 3.50 μg m^{-3}), K (average: 3.02 ± 2.29 μg m^{-3}; median: 2.47 μg m^{-3}), S (average: 2.29 ± 1.57 μg m^{-3}; median: 1.99 μg m^{-3}), Ca (average: 1.87 ± 1.36 μg m^{-3}; median: 1.73 μg m^{-3}), Na (average: 1.80 ± 1.64 μg m^{-3}; median: 1.29 μg m^{-3}), and Al (average: 1.19 ± 0.78 μg m^{-3}; median: 0.72 μg m^{-3}) that were present in major proportion, followed by Fe (average: 0.82 ± 0.51 μg m^{-3}; median: 0.78 μg m^{-3}), Zn (average: 0.49 ± 0.35 μg m^{-3}; median: 0.39 μg m^{-3}), P (average: 0.46 ± 0.43 μg m^{-3}; median: 0.15 μg m^{-3}), Pb (average: 0.43 ± 0.35 μg m^{-3}; median: 0.05 μg m^{-3}), Mg (average: 0.36 ± 0.37 μg m^{-3}; median: 0.217 μg m^{-3}), Cu (average: 0.21 ± 0.19 μg m^{-3}; median: 0.081 μg m^{-3}), Cr (average: 0.21 ± 0.14 μg m^{-3}; median: 0.195 μg m^{-3}), Mo (average: 0.20 ± 0.13 μg m^{-3}; median: 0.1 μg m^{-3}), Ti (average: 0.19 ± 0.18 μg m^{-3}; median: 0.013 μg m^{-3}), As (average: 0.19 ± 0.14 μg m^{-3}; median: 0.002 μg m^{-3}), Ni (average: 0.14 ± 0.04 μg m^{-3}; median: 0.122 μg m^{-3}), Br (average: 0.12 ± 0.11 μg m^{-3}; median: 0.07 μg m^{-3}), and Mn (average: 0.07 ± 0.07 μg m^{-3}; median: 0.009 μg m^{-3}) that were estimated in trace level (Fig. 2). Al, Na, Ca, S, Cl, and K have been identified as major elements in $PM_{2.5}$ not only in this study but also in other research leaded in Delhi (Jain et al. 2017; Rai et al. 2020a, b; Rai et al. 2021; Bangar et al. 2021). Throughout the entire sampling period (2013–2021) in Delhi, the cumulative concentrations (∑all elements) of both major and trace elements were measured at 17 ± 13 μg m^{-3} that constituted ~ 14% of the total $PM_{2.5}$ mass concentration. The research indicates that the percentage contribution of elemental composition in $PM_{2.5}$ aligns with findings from previous study conducted in Delhi (Jain et al. 2017). The maximum percentage contribution of elemental composition was reported in the year 2014, i.e. ~ 18% whereas the year 2020 have minimum contribution, i.e. ~ 9% (Table 1).

The seasonal average concentration (± SD) of $PM_{2.5}$ was observed to be highest during post-monsoon (192 ± 110 μg m^{-3}), followed by winter (158 ± 70 μg m^{-3}), summer (92 ± 44 μg m^{-3}), and monsoon (67 ± 32 μg m^{-3}) seasons (Fig. S1**;** in supplementary information). Notably, the mean concentrations of $PM_{2.5}$ during all seasons exceeded the NAAQS limit. The elevated concentrations can be attributed to various factors, including meteorological conditions and occasional burning activities (Jain et al. 2017; Sharma et al. 2020; 2022). Table 2 provides a summary of the seasonal statistics for elements such as Na, K, Mg, Ca, Al, S, Ti, Mn, Fe, Cu, Zn, As, Br, Pb, Cr, Cl, P, Mo, and Ni in relation to $PM_{2.5}$, along with their respective contributions to $PM_{2.5}$. Cl, K, S, Ca, Na, and Al were estimated as major elements in $PM_{2.5}$ samples in all seasons. The summer months (March–May) witnessed the highest percentage contribution to the total elemental composition of $PM_{2.5}$ mass, accounting for 16.9%, followed by the monsoon season (June–September) with 16.6% contribution to $PM_{2.5}$. Winter

Table 1 Annual average and overall mean elemental concentrations of $PM_{2.5}$ (μg m^{-3}) in Delhi, India

Elements (El)	2013	2014	2015	2016	2017	2018	2019	2020	2021	Mean
Na	2.97 ± 2.21	4.02 ± 3.44	3.85 ± 3.68	3.61 ± 3.41	0.76 ± 0.67	0.48 ± 0.49	0.25 ± 0.31	0.14 ± 0.21	0.11 ± 0.12	1.80 ± 1.64
K	4.85 ± 3.03	3.36 ± 1.12	3.95 ± 3.35	4.78 ± 2.33	2.21 ± 1.16	2.04 ± 2.22	2.42 ± 2.15	1.76 ± 1.53	1.82 ± 1.61	3.02 ± 2.29
Mg	0.91 ± 1.06	1.00 ± 0.85	0.30 ± 0.12	0.32 ± 0.14	0.25 ± 0.18	0.15 ± 0.19	0.15 ± 0.29	0.08 ± 0.15	0.08 ± 0.07	0.36 ± 0.37
Ca	3.69 ± 1.84	1.97 ± 2.18	2.76 ± 0.92	3.63 ± 1.27	1.71 ± 1.35	1.00 ± 1.47	1.17 ± 1.60	0.40 ± 0.50	0.53 ± 0.58	1.87 ± 1.36
Al	2.87 ± 0.93	2.22 ± 1.13	1.82 ± 0.95	1.20 ± 0.96	0.70 ± 0.55	0.55 ± 0.75	0.56 ± 0.64	0.39 ± 0.45	0.37 ± 0.35	1.19 ± 0.78
S	1.82 ± 1.62	2.48 ± 1.50	2.15 ± 1.01	2.71 ± 1.97	2.78 ± 1.82	2.03 ± 1.65	2.61 ± 1.83	1.95 ± 1.24	2.05 ± 1.23	2.29 ± 1.57
Ti	0.08 ± 0.15	0.13 ± 0.34	0.08 ± 0.04	0.09 ± 0.03	0.23 ± 0.21	0.50 ± 0.20	0.15 ± 0.05	0.32 ± 0.26	0.15 ± 0.14	0.19 ± 0.18
Mn	0.02 ± 0.02	0.01 ± 0.02	0.02 ± 0.01	0.01 ± 0.01	0.16 ± 0.15	0.11 ± 0.18	0.12 ± 0.11	0.13 ± 0.08	0.09 ± 0.05	0.07 ± 0.07
Fe	0.26 ± 0.40	0.38 ± 0.52	0.99 ± 0.50	1.11 ± 0.37	1.02 ± 0.56	1.21 ± 0.78	0.81 ± 0.48	0.71 ± 0.43	0.87 ± 0.59	0.82 ± 0.51
Cu	0.05 ± 0.12	0.10 ± 0.23	0.09 ± 0.06	0.16 ± 0.16	0.35 ± 0.25	0.43 ± 0.28	0.19 ± 0.14	0.21 ± 0.12	0.29 ± 0.18	0.21 ± 0.19
Zn	0.12 ± 0.20	0.22 ± 0.29	0.45 ± 0.27	0.54 ± 0.34	0.69 ± 0.49	0.98 ± 0.48	0.52 ± 0.36	0.41 ± 0.29	0.48 ± 0.36	0.49 ± 0.35
As	0.06 ± 0.16	0.10 ± 0.17	0.10 ± 0.14	0.11 ± 0.12	0.21 ± 0.13	0.37 ± 0.13	0.19 ± 0.11	0.23 ± 0.11	0.31 ± 0.12	0.19 ± 0.14
Br	0.03 ± 0.12	0.05 ± 0.09	0.09 ± 0.07	0.11 ± 0.08	0.16 ± 0.10	0.35 ± 0.38	0.08 ± 0.08	0.11 ± 0.10	0.10 ± 0.07	0.12 ± 0.11
Pb	0.02 ± 0.03	0.14 ± 0.22	0.37 ± 0.28	0.47 ± 0.26	0.18 ± 0.13	0.35 ± 0.26	0.66 ± 0.34	0.73 ± 0.48	0.91 ± 0.48	0.43 ± 0.35
Cr	0.17 ± 0.14	0.14 ± 0.15	0.19 ± 0.11	0.21 ± 0.13	0.19 ± 0.09	0.30 ± 0.18	0.21 ± 0.08	0.22 ± 0.14	0.30 ± 0.17	0.21 ± 0.14
Cl	4.69 ± 2.27	3.40 ± 2.21	5.14 ± 3.99	5.48 ± 2.95	2.57 ± 2.73	1.92 ± 2.36	2.24 ± 2.55	2.32 ± 2.49	2.21 ± 2.08	3.44 ± 2.68
P	1.05 ± 0.84	0.74 ± 0.44	0.99 ± 1.02	1.01 ± 0.60	0.11 ± 0.13	0.13 ± 0.24	0.07 ± 0.06	0.05 ± 0.13	0.03 ± 0.02	0.46 ± 0.43
Mo	0.09 ± 0.07	0.16 ± 0.17	0.27 ± 0.16	0.35 ± 0.17	0.18 ± 0.08	0.19 ± 0.18	0.12 ± 0.04	0.18 ± 0.09	0.25 ± 0.13	0.20 ± 0.13
Ni	–	–	–	–	0.15 ± 0.06	0.13 ± 0.02	0.12 ± 0.02	0.13 ± 0.03	0.16 ± 0.03	0.14 ± 0.04
∑ El	23.74	20.61	23.61	25.90	14.61	13.21	12.64	10.49	11.09	17.49
$PM_{2.5}$	136 ± 91	113 ± 96	123 ± 65	138 ± 58	143 ± 70	124 ± 70	129 ± 96	116 ± 68	109 ± 53	126 ± 77
% of ∑El in $PM_{2.5}$	17.5%	18.2%	19.2%	18.8%	10.2%	10.7%	9.8%	9.0%	10.2%	13.9%

± standard variation (SD at 1σ)

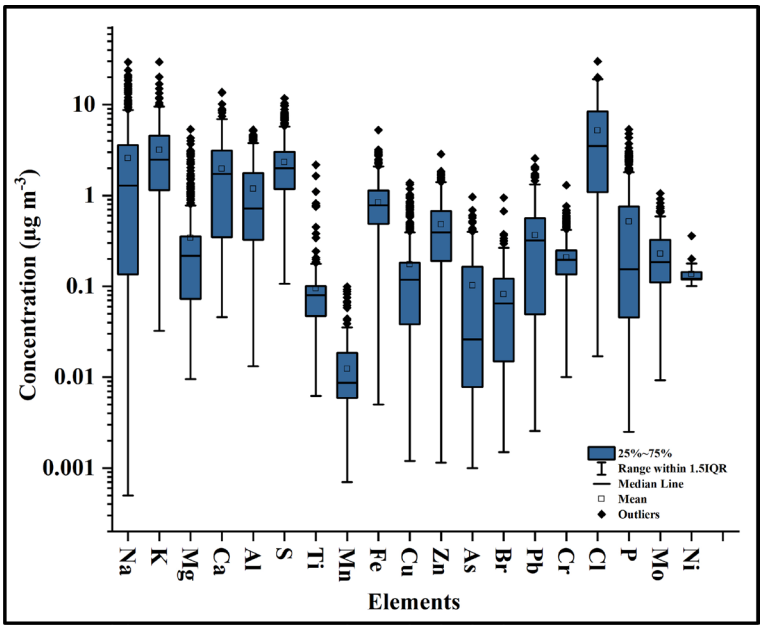

Fig. 2 Box plot for annual elemental concentrations of $PM_{2.5}$ from the year 2013–2021

months (January–February) exhibited a 12.9% contribution to $PM_{2.5}$, and the post-monsoon period (October–December) contributed 11.7% to the total elemental composition of $PM_{2.5}$ mass (Table 2). During the winter months (January–February), key contributors to $PM_{2.5}$ concentration included Cl (5.19 ± 4.13 μg m^{-3}), K (3.40 ± 2.60 μg m^{-3}), S (2.66 ± 1.18 μg m^{-3}), Na (1.95 ± 2.17 μg m^{-3}), Ca (1.86 1.97 μg m^{-3}), and Al (1.24 ± 1.31 μg m^{-3}), collectively representing 80% of the total elemental contribution. In contrast, the summer period (March–May) witnessed substantial contributions from K (2.70 ± 1.82 μg m^{-3}), Cl (2.70 ± 2.35 μg m^{-3}), Ca (2.37 ± 1.59 μg m^{-3}), S (1.66 ± 1.02 μg m^{-3}), Na (1.55 ± 1.41 μg m^{-3}), and Al (1.17 ± 0.94 μg m^{-3}), comprising 78% of the total elemental contribution to $PM_{2.5}$ concentrations. Transitioning into the monsoon months (June–September), significant contributors were K (1.83 ± 1.98 μg m^{-3}), Ca (1.83 ± 1.70 μg m^{-3}), S (1.62 ± 0.98 μg m^{-3}), Na (1.18 ± 1.17 μg m^{-3}), and Cl (1.03 ± 1.69 μg m^{-3}), accounting for 67% of the total elemental contribution to $PM_{2.5}$ mass loadings. In the post-monsoon season (October–December), Cl (4.79 ± 4.55 μg m^{-3}), K (4.61 ± 3.02 μg m^{-3}), S (3.30 ± 2.11 μg m^{-3}), Ca (1.97 ± 1.94 μg m^{-3}), Na (1.86 ± 2.10 μg m^{-3}), and Al (1.41 ± 1.23 μg m^{-3}) emerged as major contributors, constituting 80% of the total elemental contribution to $PM_{2.5}$ concentrations. The increased presence of Cl in $PM_{2.5}$ samples at the time of winter, and post-monsoon seasons can be attributed to activities such as combustion and biomass burning (Singhal et al. 2017; Chang et al. 2018), whereas the elevated concentration of K during summer and monsoon seasons may be associated with combustion, crustal and road dust related activities (Jain et al. 2017; Sharma et al. 2022). The consistent observation of Al, Ca, and Na in $PM_{2.5}$ throughout all seasons suggests a contribution from mineral and soil dust to the $PM_{2.5}$ mass loading. The sources of crustal, soil, and road dust in $PM_{2.5}$ at the sampling site may stem from both local and long-range transportation of pollutants, including those from deserts, paved or unpaved roads, as well as construction and agricultural activities (Sharma et al. 2014; Jain et al. 2020a, b; Bangar et al. 2021).

Impact of Air Mass Backward Trajectories on $PM_{2.5}$

In order to understand the trajectories of particulate air masses reaching the sampling site, Delhi, seasonal trajectories at 500 m above the ground level (AGL) were generated, as depicted in Fig. S4 (in supplementary information). During the winter season, the backward trajectories of atmospheric masses reaching to Delhi originated locally and from states including Punjab, Haryana, Uttar Pradesh, Rajasthan, Gujarat, West Bengal, Bihar, some parts of Madhya Pradesh, and northern states like Himachal Pradesh and Jammu and Kashmir. Additionally, contributions came from neighbouring countries such as Pakistan, Afghanistan, Iran, and Nepal. In the summer season, the backward air parcels were traced back to Maharashtra, Andhra Pradesh, West Bengal, Rajasthan, Gujarat, Punjab, Haryana, Bihar, Uttar Pradesh, Uttarakhand, Himachal Pradesh, some parts of Madhya Pradesh, the Arabian Sea, the Bay of Bengal, and countries including Pakistan, Afghanistan, Iran, Tajikistan, Bangladesh, and Nepal. Throughout the monsoon season, the predominant air flow originated from the Arabian Sea and the Bay of Bengal. Additionally, contributions were observed from regional states such as Maharashtra,

Table 2 Annual mean and overall mean elemental concentrations of $PM_{2.5}$ (μg m^{-3}) in Delhi, India

Elements (El)	Winter ($n=161$)	Summer ($n=181$)	Monsoon ($n=199$)	Post-monsoon ($n=215$)
Na	1.95 ± 2.17	1.55 ± 1.41	1.18 ± 1.17	1.86 ± 2.10
	(0.02–21.18)	(0.01–17.04)	(0.01–18.68)	(0.02–29.41)
K	3.40 ± 2.60	2.70 ± 1.82	1.83 ± 1.98	4.61 ± 3.02
	(0.17–20.15)	(0.08–5.55)	(0.03–8.61)	(0.36–14.99)
Mg	0.24 ± 0.40	0.29 ± 0.22	0.37 ± 0.47	0.45 ± 0.78
	(0.01–2.86)	(0.01–1.51)	(0.02–3.04)	(0.02–5.35)
Ca	1.86 ± 1.97	2.37 ± 1.59	1.83 ± 1.70	1.97 ± 1.94
	(0.06–13.71)	(0.12–8.13)	(0.05–8.94)	(0.05–10.14)
Al	1.24 ± 1.31	1.17 ± 0.94	0.91 ± 0.86	1.41 ± 1.23
	(0.01–5.27)	(0.06–4.02)	(0.08–5.15)	(0.06–5.27)
S	2.66 ± 1.18	1.66 ± 1.02	1.62 ± 0.98	3.30 ± 2.11
	(0.56–7.00)	(0.11–4.77)	(0.15–6.10)	(0.14–10.72)
Ti	0.09 ± 0.08	0.11 ± 0.21	0.09 ± 0.14	0.15 ± 0.21
	(0.02–0.75)	(0.01–0.59)	(0.01–1.10)	(0.01–1.64)
Mn	0.06 ± 0.11	0.04 ± 0.06	0.10 ± 0.13	0.07 ± 0.08
	(0.01–0.92)	(0.01–0.39)	(0.002–0.75)	(0.002–0.68)
Fe	0.85 ± 0.46	0.83 ± 0.60	0.71 ± 0.57	0.95 ± 0.59
	(0.01–2.34)	(0.01–2.98)	(0.01–5.25)	(0.02–3.19)
Cu	0.21 ± 0.23	0.16 ± 0.20	0.12 ± 0.17	0.21 ± 0.22
	(0.01–1.38)	(0.01–1.32)	(0.002–1.19)	(0.01–1.03)
Zn	0.60 ± 0.39	0.44 ± 0.35	0.26 ± 0.25	0.64 ± 0.43
	(0.02–1.85)	(0.01–1.85)	(0.01–1.49)	(0.02–2.86)
As	0.18 ± 0.15	0.07 ± 0.12	0.03 ± 0.05	0.18 ± 0.17
	(0.01–0.59)	(0.01–0.69)	(0.01–0.35)	(0.003–0.96)
Br	0.12 ± 0.12	0.11 ± 0.23	0.09 ± 0.08	0.13 ± 0.11
	(0.01–0.86)	(0.01–1.95)	(0.01–0.50)	(0.01–0.94)
Pb	0.41 ± 0.34	0.24 ± 0.25	0.26 ± 0.29	0.52 ± 0.46
	(0.01–1.57)	(0.01–1.05)	(0.01–1.64)	(0.02–2.56)
Cr	0.27 ± 0.16	0.20 ± 0.14	0.13 ± 0.07	0.24 ± 0.12
	(0.03–1.60)	(0.01–0.69)	(0.02–0.29)	(0.02–0.76)
Cl	5.19 ± 4.13	2.70 ± 2.35	1.03 ± 1.69	4.79 ± 4.55
	(0.28–19.38)	(0.13–19.05)	(0.11–18.72)	(0.13–29.95)
P	0.68 ± 0.89	0.56 ± 0.63	0.35 ± 0.56	0.51 ± 0.69
	(0.01–5.35)	(0.02–3.06)	(0.01–4.80)	(0.01–3.72)
Mo	0.29 ± 0.19	0.20 ± 0.15	0.15 ± 0.11	0.28 ± 0.16
	(0.03–0.91)	(0.01–0.65)	(0.01–0.68)	(0.03–1.05)
Ni	0.13 ± 0.02	0.15 ± 0.07	0.12 ± 0.02	0.14 ± 0.03
	(0.10–0.21)	(0.11–0.36)	(0.11–0.15)	(0.11–0.21)
∑ El	20.42 ± 16.9	15.53 ± 12.36	11.14	22.38 ± 19.00
$PM_{2.5}$	158 ± 70	92 ± 44	67 ± 32	192 ± 110
% of ∑El in $PM_{2.5}$	12.9%	16.9%	16.6%	11.7%

± standard variation (at 1σ); value in parentheses is range (min –max)

winter: JF; summer: MAM; monsoon: JJAS; post-monsoon: OND

Madhya Pradesh, West Bengal, Rajasthan, Gujarat, Punjab, Haryana, Bihar, Uttar Pradesh, Uttarakhand, Himachal Pradesh, as well as countries including Bangladesh, Burma, Uzbekistan, and Nepal. In the post-monsoon period, the maximum air flow originated from the western part of India, encompassing the Arabian Sea, Rajasthan, Gujarat, Haryana, and Punjab. Some air parcels also originated from Uttar Pradesh, West Bengal, and Nepal. To identify the likely source regions of $PM_{2.5}$ at the receptor site, Delhi, a potential source contribution function (PSCF) analysis was conducted. Grids exhibiting a probability below 0.1 were made transparent, and the remaining grids were presented

in a spectrum of colours. Lighter shades represented lower probabilities, while darker hues indicated higher probabilities. In the winter season, noteworthy air mass loads with higher WPSCF values (> 0.9) originated locally at specific sites (Anand Vihar, Kashmiri Gate, Ghaziabad, Kirti Nagar, Patel Nagar, Rajendra Place). WPSCF values ranging from 0.3 to 0.9 were observed in regional states like Haryana and Punjab, attributed to various burning activities conducted for heating purposes. Additionally, WPSCF values in the range of 0.1 to 0.2 were associated with both regional and trans-boundary sources, including Jammu & Kashmir, Uttar Pradesh, Rajasthan, Pakistan, Afghanistan, and Nepal (Fig. 3). During the summer season, heightened loadings of $PM_{2.5}$ with WPSCF values > 0.9 were found to originate locally, while values in the range of 0.3–0.9 originated from Punjab, Haryana, and specific areas of Uttarakhand and Himachal Pradesh. Lower WPSCF values (0.1–0.2) were associated with both regional and trans-boundary sources, including the Arabian Sea, the Bay of Bengal, and countries such as Pakistan, Afghanistan, Iran, Tajikistan, Bangladesh, and Nepal (Fig. 3). In the monsoon season, substantial air masses with WPSCF values > 0.8 or in the range of 0.3 to 0.8 were primarily generated locally. Lower WPSCF values (0.1–0.2) were linked to both regional and trans-boundary sources, encompassing the Arabian Sea, the Bay of Bengal, Maharashtra, Madhya Pradesh, West Bengal, Rajasthan, Gujarat, Punjab, Haryana, Bihar, Uttar Pradesh, Uttarakhand, Himachal Pradesh, and countries such as Bangladesh, Burma, Uzbekistan, and Nepal (Fig. 3). In the post-monsoon period, the predominant air flow with WPSCF values > 1.0 originated locally, while values in the range of 0.3–0.9 were traced back to Haryana and Punjab, attributed to occasional burning activities like stubble burning during this season (Jain et al. 2017). Lower WPSCF values (0.1–0.2) were associated with both regional and trans-boundary sources, including the Arabian Sea, Rajasthan, and Gujarat (Fig. 3) (Naja et al. 2014; Jain et al. 2017, 2021). The seasonal backward trajectory analysis at different heights, i.e. 1000 m and 1500 m AGL for 120 h, was also plotted and analysed (Fig. S5–S6, in supplementary information). There is no potential impact of varying trajectory heights on air parcel results. Furthermore, the seasonal PSCF analysis is detailed in the supplementary information (Fig. S7–S8, in supplementary information), indicating minimal variation in the results.

Conditional Bivariate Probability Function

To gain a deeper understanding of the directional influence of local sources, a seasonal conditional bivariate polar function (CBPF) plot was executed for the Delhi sampling site (Uria-Tellaetxe et al. 2014) (Fig. 4). In the winter season, programmed wind speed (WS) ranging from approximately 0.21–2.00 m/s, coupled with mass concentrations (> 75th percentile, 158 μg m^{-3}), indicated a major source region in the centre, possibly attributed to traffic emissions, given the proximity to traffic junctions (Patel Nagar, Rajendra Place, Shadipur). The south–east (S–E) direction revealed a heavy traffic region (Daryaganj, Saket, CP, Anand Vihar terminal), while the south–west (S–W) direction suggested emissions from nearby industries, particularly the Naraina industrial area. In the summer season, programmed WS approximately ranging from 0.23 to 2.29 m/s, coupled with mass concentrations (> 75th percentile, 92 μg m^{-3}), identified the major source region in the south–west (S–W) direction, indicating industrial emissions from metal processing industries in the Naraina industrial area. The central region also showed

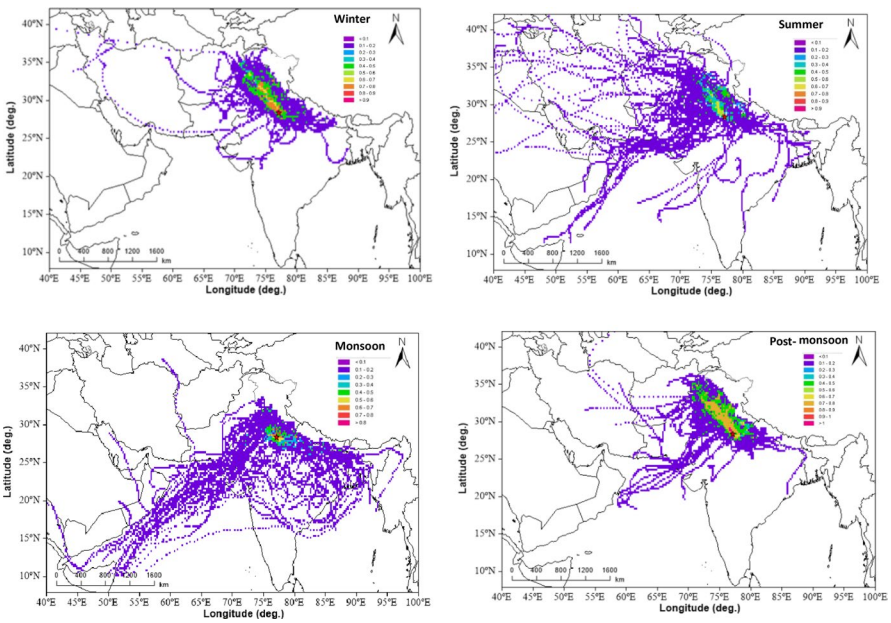

Fig. 3 Seasonal air mass PSCF analysis of $PM_{2.5}$ at height 500 m (AGL) over Delhi

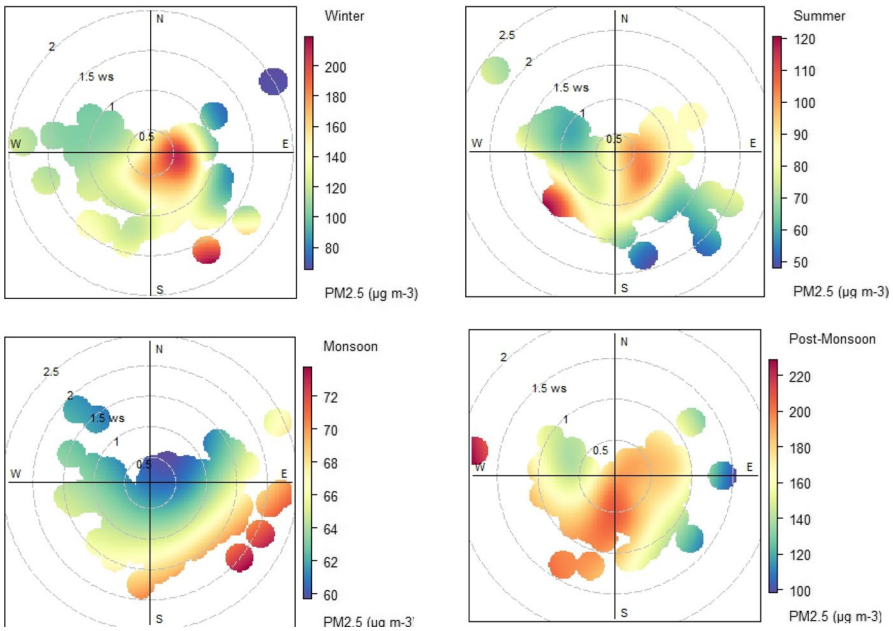

Fig. 4 Seasonal CBPF plots for Delhi

potential traffic-related contributions from surrounding junctions (Patel Nagar, Rajendra Place, Shadipur). During the monsoon season, programmed WS approximately ranging from 0.08 to 2.40 m/s, with mass concentrations (> 75th percentile, 67 µg m^{-3}), pointed towards the major source regions in the south (S) and south–west (S–W) directions. This suggested contributions from industrial emissions in the Naraina industrial area and traffic emissions from the southern part of Delhi. In the post-monsoon period, programmed WS approximately ranging from 0.06 to 1.80 m/s, with mass concentrations (> 75th percentile, 192 µg m^{-3}), indicated major source regions in the north–west (N–W), south–west (S–W), south (S), and central areas. Contributions from traffic emissions near junctions (Patel Nagar, Rajendra Place, Shadipur) in the central region were noted, along with potential contributions from agriculture fields (ICAR-Indian Agricultural Research Institute), forests (Central Ridge Forest), and residential areas surrounding the site. The north–west (N–W) direction indicated industrial emissions and combustion activities (open waste burning, heating purposes) in areas such as Rohini, Kanjhawala, Narela, and Bawana (Jain et al. 2019; Shivani et al. 2019; Rai et al. 2020a, b; Banoo et al. 2020, 2024).

Source Apportionment: Annual Source Profiles of $PM_{2.5}$ on Long-Term basis

Positive matrix factorization (PMF 5.0 version) was employed to discern additional source details for the elements in $PM_{2.5}$. In the annual period spanning 2013 to 2021, a seven-factor solution was chosen as the most reliable, utilizing 18 species (Na, K, Mg, Ca, Al, S, Ti, Mn, Fe, Cu, Zn, As, Br, Pb, Cr, Cl, P, and Mo) and 756 $PM_{2.5}$ samples with Ti as a weak species and extra modelling uncertainty of 16.5%. The source profiles and % contribution identified by the PMF analysis are shown in Fig. 5 (Table S5-S6, in supplementary information). Seven factors, i.e. two dust related factors (crustal/road dust, and paved road dust), Br-rich, combustion, vehicular emissions, and biomass burning and industrial emissions, were estimated for $PM_{2.5}$ for the years 2013–2021.

Dust

The PMF analysis revealed two factors related to dust, encompassing crustal/soil/road dust (rich in Na and Al) and paved road dust (rich in Mg, Ca, and Fe), contributing 15.7% and 14.2%, respectively. Crustal and road dust with higher loadings for Na (52%), K (30%), Mg (36%), Ca (38%), and Al (64%) while paved roads have higher loadings for Mg (51%), Ca (53%), and Fe (50%). The two dust related factors together explained 91% of Ca and 87% of Mg while the other factors explained only 9% of Ca and 13% of Mg. Several other researchers reference these elements (Ca, Na, Mg, K, and Al) as indicative of a soil/crustal/dust source (Gugamsetty et al. 2012; Waked et al. 2014; Khan et al. 2016; Jeong et al. 2017; Manousakas et al. 2022). A comprehensive set of marker elements employed in India for the identification of soil dust comprises Al, Si, Ca, Ti, Fe, Pb, Cu, Cr, Ni, Co, and Mn (Gupta et al. 2012; Banerjee et al. 2015; Sharma et al. 2016b; Jain et al. 2017). The elevated relative contributions of Ca in road dust have been identified in other source apportionment studies; generally, Ca and Mg are frequently linked to mineral dust and construction activities (Bukowiecki et al.

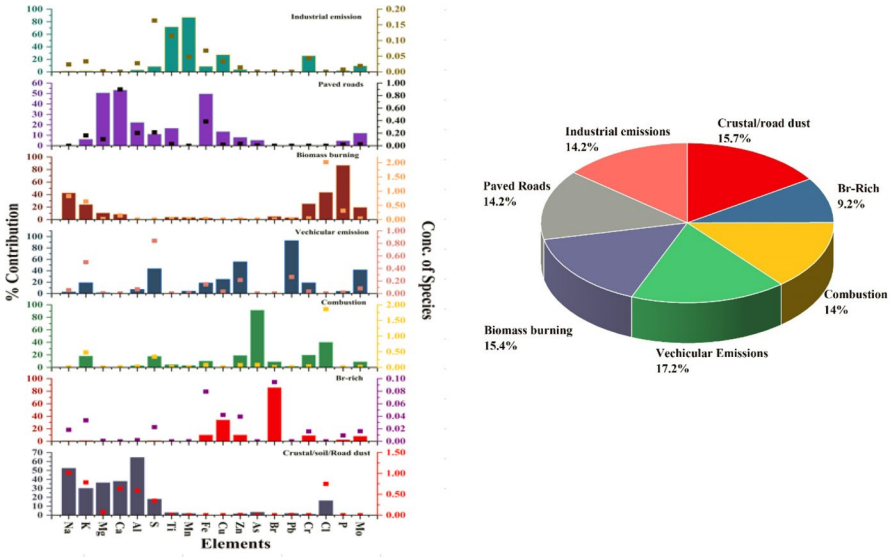

Fig. 5 Annual (2013–2021) source profiles and % source contribution of $PM_{2.5}$ extracted by PMF

2010; Crilley et al. 2016; Maenhaut 2017; Rai et al. 2020a, b). The sampling site's proximity to the freeway suggests susceptibility to the wear and tear of asphalt and concrete roads, primarily due to heavy traffic influence. The increased proportion of crustal elements like Ca and Mg in road dust could result from the extensive use of asphalt and concrete in road construction (Fullova et al. 2017).

Br-rich

The second factor was identified as Br-rich source (9%) of $PM_{2.5}$, with a sole contribution consisting of 86% of Br. This factor also includes Cu with 34% of contribution. According to the previous studies there are various sources like refuse burning that includes biomass burning, vehicular emissions, waste incineration related activities, industrial emissions, etc. releases Br into the atmosphere (Karar and Gupta 2007; Chelani et al. 2010; Gugamsetty et al. 2012; Chen et al. 2018; Liao et al. 2021; Peng et al. 2021). Apart from combustion-related activities, bromine (Br) is also emitted from sources such as soil dust, geothermal steams, sea spray, and wastewater treatment plants, as noted by Leri et al. (2024). In this context, sources rich in Br are considered a mixed type source of $PM_{2.5}$.

Combustion

The factor three was identified as combustion and this factor contributed 14% to the $PM_{2.5}$ mass having higher loadings of As (91%) and Cl (40%). Several previous researches suggested that As and Cl are the major contributor to the coal combustion (Jiang et al. 2018; Dai et al. 2020). Also, As and Cl were emitted through traffic emission mostly through fuel combustion (Dai et al. 2020). As is also a marker for industrial combustion process mostly in metal manufacturing plants (Chen et al. 2018).

Vehicular Emissions

This traffic-related emissions or vehicular emissions (both exhaust and non-exhaust) serves as a fourth factor that contributed 17.2% to the total $PM_{2.5}$ mass and have higher loadings for S (44%), Zn (56%), Pb (93%), and Mo (41%). The elements Zn, Pb, and Mo mostly emitted through non-exhaust vehicular activities such as brake and tire wear (Khan et al. 2016; Prakash et al. 2018; Jiang et al. 2018). This factor solely explained 93% contribution of Pb in total $PM_{2.5}$ mass composition that is a tracer for wearing of vehicle tires (Prakash et al. 2018). Zn and Mo are prevalent trace elements found in abundance in brake pads and brake linings. These elements are commonly associated with tire and brake wear (Grigoratos and Martini 2015; Khan et al. 2016; Jiang et al. 2018). S is a component emitted through exhaust vehicular emissions (fuel combustion) (Amato et al. 2009). S can be present in vehicular emissions, primarily in the form of SO_2 and sulphur-containing compounds. The ignition of fossil fuels, such as gasoline and diesel, releases sulphur compounds into the atmosphere (Jain et al. 2019; Saraswati et al. 2019; Choudhary et al. 2023).

Biomass burning

The PMF analysis reveals the fifth factor as biomass burning that contributed 15.4% for $PM_{2.5}$ mass composition having higher loadings for P (87%), Cl (44%), Na (43%), and K (24%). Previous studies reveal the emission of Na and Cl through biomass burning emissions from open agricultural residue burning (Singhal et al. 2017). In the context of

particulate matter (PM) in India, K has been utilized as a primary indicator for the identification of biomass burning (Ram et al. 2010). Situated in close proximity to an agricultural area, the sampling site is encircled by regions engaged in various agricultural activities, including burning practices. This proximity increases the likelihood of phosphorus in $PM_{2.5}$ samples. Biomass burning, whether from agricultural residue burning or forest fires, can release phosphorus into the atmosphere. Plant materials contain phosphorus, and when burned, it can be emitted as PM (Akagi et al. 2011; Bhuvaneshwari et al. 2019; Meng et al. 2022).

Industrial Emissions

The elevated presence of Mn (87%), Ti (72%), Cu (27%), and Cr (26%) characterizes industrial emissions, likely originating from nearby metal manufacturing plants and storage facilities situated in close proximity to the sampling site. A suite of marker species, including Co, Cd, Zn, Ni, Cr, Mn, S, As, Fe, Cu, and Mo, has been employed in India to discern specific industrial emissions (Banerjee et al. 2015; Sharma et al. 2014). Ti is emitted as TiO_2 that is a tracer for dust related emissions, and also, it is used in ore mining activities which is coming from long-range transport (Jain et al. 2019). In the current study, PMF analysis identified a 14.2% contribution to $PM_{2.5}$ mass from industrial emissions.

The seasonal sources of $PM_{2.5}$ were also examined using PMF and extracted seasonal sources are available in supplementary information (Supplementary Text 1; Fig. S10-S13).

Health Risk

Despite the fact that trace/heavy elements only account for a small percentage of $PM_{2.5}$'s total mass concentration, their non-degradable nature and accessibility raise serious concerns for human health (Li et al. 2023). Comprehending the manner in which $PM_{2.5}$ affects health necessitates an understanding of the intricate interactions between oxidative stress, cellular damage, systemic effects, and inflammatory responses (Saffari et al. 2014; Lopez Cruz et al. 2016; Prakash et al. 2018). In order to assess the health risks connected to trace elements, they must be divided into categories: carcinogenic and non-carcinogenic. Based on estimated element levels of the years 2013–2021, the health risks were computed annually and seasonally in order to evaluate how emission control measures affected element concentrations (Table S15; in supplementary information).

Annually, the non-carcinogenic risks linked with trace/heavy elements. The HQ values of Cr (2×10^{0} (adult) and 4.7×10^{0} (child)) and Mn (1.4×10^{0} (adult) and 3.2×10^{0} (child)) comparing to other elements, showed elevated values on an annual basis (Fig. 6). The HQ values for other elements were below one, indicating that elements did not appear to be a non-carcinogenic risk overall. Furthermore, the combined HQ value of these elements, i.e. HI (Hazard Index) is greater than one, suggesting that there is appreciable non-carcinogenic risk connected to the elements (Li et al. 2023). In terms of carcinogenic risks (CR), the order of CR values for adults and children has been calculated by utilizing the concentrations of trace/heavy elements as- Cr (4.2×10^{-4}) and (1.0×10^{-4}) > As (4.9×10^{-5}) and (1.2×10^{-5}) > Pb (4.5×10^{-7}) and (1.1×10^{-7}) > Ni (2.5×10^{-7}) and (6.2×10^{-8}), respectively. Adults and children had cumulative CR values of 4.7×10^{-4} and 1.12×10^{-4}, respectively. Notably, Cr exceeded the USEPA's allowable limit and demonstrated a carcinogenic effect in both adults and children.

In addition to conducting annual assessment of health risk, we also computed the seasonal health risk assessment for carcinogenic and non-carcinogenic effects for the years 2013–2021 in Delhi (Fig. 7). In winter, the non-carcinogenic risk associated with trace/heavy elements showed elevated HQ values for Cr (2.5×10^{0} (adult), 5.8×10^{0} (child)) and Mn (1.3×10^{0} (adult), 3.1×10^{0} (child)) comparing to other elements. The carcinogenic risk (CR) values were also calculated and found higher for Cr ((5.1×10^{-4}) and (1.3×10^{-4})) in both adults and children respectively. The exceeded values of Cr demonstrated a carcinogenic effect in both adults and children. Similarly, in summer the non-carcinogenic risk showed elevated HQ

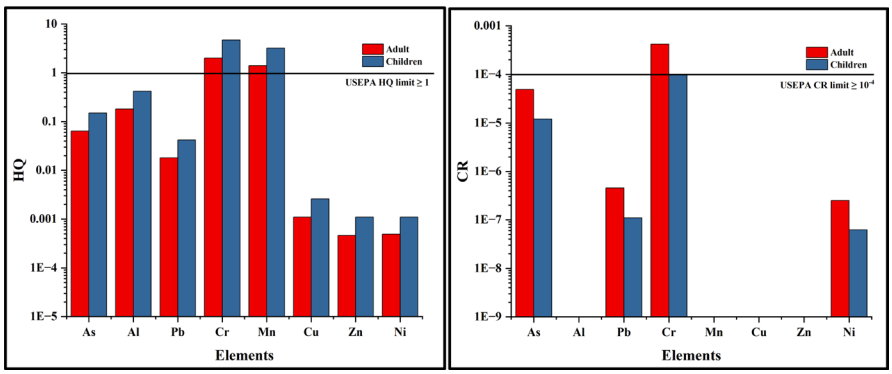

Fig. 6 Annual assessment of hazard quotient (HQ), and carcinogenic risk (CR) of heavy elements in Delhi

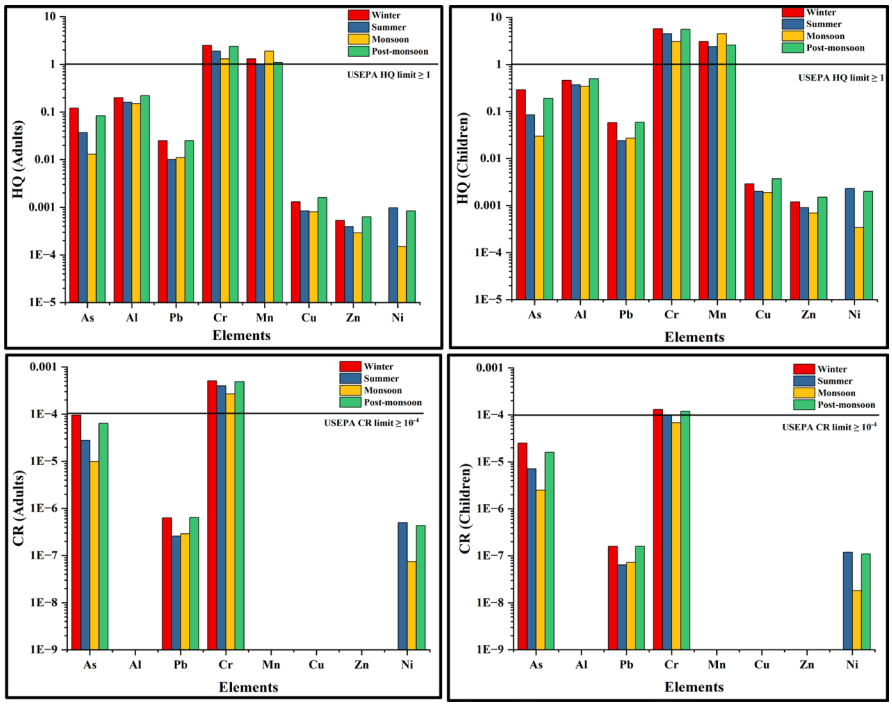

Fig. 7 Seasonal assessment of Hazard Quotient (HQ), and Carcinogenic Risk (CR) of heavy elements in Delhi

values for Cr (1.9×10^{0} (adult) 4.5×10^{0}(child)) and Mn (1.0×10^{0}(adult) 2.4×10^{0}(child)) comparing to other elements. The carcinogenic risk (CR) values evaluated by using concentration of trace/heavy elements found to be in the accepted range for children as provided by USEPA, but for adults the CR values of Cr showed value 4.0×10^{-4} exceeded from the limit. In monsoon, the non-carcinogenic risk associated with trace/heavy elements showed elevated HQ values for Cr (1.3×10^{0} (adult) 3.1×10^{0}(child)) and Mn (1.9×10^{0}(adult) 4.5×10^{0}(child)) comparing to other elements. Like summer, also in monsoon the CR values for Cr found to be in the accepted range for children and for adults it is found to be 2.7×10^{-4}. Succeeding to this, in post-monsoon season the non-carcinogenic risk of trace/heavy elements showed higher HQ values for Cr (2.4×10^{0} (adult), 5.6×10^{0} (child)) and Mn (1.1×10^{0} (adult), 2.6×10^{0} (child)) in comparison to other elements. The carcinogenic risk (CR) values calculated using concentration of trace elements and found to be exceeded for Cr 4.9×10^{-4} (adult) 1.2×10^{-4} (child). Previous researchers also reported the carcinogenic risk of Cr, Mn, As, Ni and Pb of $PM_{2.5}$ exposures in Delhi and other nearby areas (Agarwal et al. 2017; Prakash et al. 2018; Sah 2022; Singh et al. 2023). Also, various researchers internationally reported the carcinogenic risk of Pb, As, Sn, Cd, Zn and Ni of $PM_{2.5}$ outside India (Li et al. 2023; Chen et al. 2021; Duan et al. 2021). Prakash et al. 2018 investigated carcinogenic risk in Delhi and reported significantly elevated health risks associated with $PM_{1.0}$-bound elements, particularly for Cr and Ni, exceeding safe limits for children and approaching tolerable limits for adults. Also, Sah (2022) reported the carcinogenic risks linked to As, Cr, and Ni were found to exceed the precautionary criterion (1×10^{-6}) for both adults and children. This suggested that there are considerable and should not be disregarded carcinogenic risks associated with exposure to these elements through $PM_{2.5}$. The carcinogenic risks associated with $PM_{2.5}$ exposure of Cd were found to be non-negligible, as evidenced by the fact that they exceeded the precautionary criterion (1×10^{-6}) for adults.

There is no significant effect of the elements exhibited carcinogenic or non-carcinogenic effects. However, Cr and Mn continued to indicate relatively adverse health impacts in both adults and children, attributed to their elevated hazard quotient (HQ) values. Additionally, high carcinogenic risk values were observed for Cr in both adults and children during the winter and post-monsoon seasons, and in adults during the summer and monsoon seasons. The higher risks associated with Cr and Mn in Delhi were hypothesized to be primarily influenced by industrial or vehicular activities. This assumption is based on the recognition that both Cr and Mn in $PM_{2.5}$ are commonly acknowledged as markers for emissions originating from industrial and vehicular sources (Gugamsetty et al. 2012; Srimuruganandam and Nagendra 2012; Belis et al. 2013; Bannerjee et al. 2015).

Conclusion

This comprehensive study conducted from January 2013 to December 2021 offers a thorough examination of $PM_{2.5}$ elemental compositions in Delhi, India, focusing on seasonal variations, long-term annual concentrations, source apportionment using PMF of elements present in $PM_{2.5}$, and health risk assessment related to heavy elements. Over the study period, 19 elements (Al, Fe, Zn, Mn, Ti, Cu, Cr, Ni, Cl, P, S, K, Mo, Na, Mg, Ca, Pb, As, and Br), comprising 13.9% of the $PM_{2.5}$ mass concentration (127 ± 77 μg m $^{-3}$), were identified in $PM_{2.5}$. The seasonal analysis consistently revealed heightened $PM_{2.5}$ concentrations, peaking during the post-monsoon period (192 ± 110 μg m $^{-3}$), followed by winter (158 ± 70 μg m $^{-3}$), summer (92 ± 44 μg m $^{-3}$), and monsoon (67 ± 32 μg m $^{-3}$), all surpassing NAAQS limits. Source apportionment identified six primary sources contributing to $PM_{2.5}$, including dust (two dust related factors), combustion, vehicular emissions, industrial emissions, Br-rich sources, and biomass burning, with varying contributions across seasons. Trajectory analysis highlighted trans-boundary origins of $PM_{2.5}$ from Afghanistan, Pakistan, Nepal, and Iran, alongside regional contributions from northern and western states of India, while CBPF analysis pinpointed local source regions in the south-east and south-west directions of Delhi. Health risk assessment uncovered heightened carcinogenic risks linked to Cr in both adults and children during winter and post-monsoon seasons, as well as in adults during summer and monsoon seasons, suggesting significant contributions from industrial or vehicular activities to the elevated risks associated with Cr and Mn in Delhi. As research in this field continues to unravel the intricate mechanisms through which $PM_{2.5}$ impacts health, the findings of this long-term elemental composition analysis offer crucial insights essential for informing public health policies and strategies aimed at reducing the health risks associated with air pollution. This long-term study on $PM_{2.5}$ composition stands as a valuable resource for policymakers dedicated to mitigating and enhancing ambient air quality and human health in Delhi and similar urban settings.

Supplementary Information The online version contains supplementary material available at https://doi.org/10.1007/s00244-024-01070-0.

Acknowledgements The authors are thankful to the Director, CSIR-NPL, and the Head, Environmental Sciences and Biomedical Metrology Division (ES&BMD), CSIR-NPL, New Delhi, for their encouragement and support for this study. Authors are also thankful to Saraswati, Srishti Jain, Rubiya Banoo, Martina Rani, and Akansha Rai for $PM_{2.5}$ samples collection. The authors thankfully acknowledge the Central Pollution Control Board (CPCB), New Delhi, for meteorological data (https://cpcb.nic.in). The authors thankfully acknowledge the NOAA Air Resources Laboratory for downloading the air mass trajectories (https://www.ready.noaa.gov/hypub-bin/trajsrcm.pl; accessed on 10–15 January 2024) datasets.

Author Contributions Sakshi Gupta contributed to data analysis, data interpretation, visualization, original draft—writing, and editing; Sudhir Kumar Sharma contributed to conceptualization and design of the study, data interpretation, fund acquisition, writing, editing, and reviewing; Preeti Tiwari contributed to data analysis, visualization, writing, and editing; Narayanasamy Vijayan contributed to resources, data interpretation, editing, and reviewing. All authors have read and agreed to the published version of the manuscript.

Funding The authors acknowledged the CSIR-National Physical Laboratory, New Delhi, India, for providing financial support for this study (OLP-230332). Authors (SG and PT) also acknowledge the UGC, New Delhi, for providing the research fellowship.

Data Availability The datasets developed during the current study are available from the corresponding author on reasonable request.

Declarations

Conflict of interest The authors declare that they have no conflict of interest.

Ethical Approval Not applicable.

Consent to Participate Not applicable.

Consent to Publish Not applicable.

References

Agarwal A, Mangal A, Satsangi A, Lakhani A, Kumari KM (2017) Characterization, sources and health risk analysis of $PM_{2.5}$ bound metals during foggy and non-foggy days in sub-urban atmosphere of Agra. Atmos Res 197:121–131

Akagi SK, Yokelson RJ, Wiedinmyer C, Alvarado MJ, Reid JS et al (2011) Emission factors for open and domestic biomass burning for use in atmospheric models. Atmos Chem Phys 11:4039–4072

Amato F, Pandolfi M, Escrig A, Querol X, Alastuey A, Pey J, Perez N, Hopke PK (2009) Quantifying road dust resuspension in urban environment by multilinear engine: a comparison with PMF2. Atmos Environ 43(17):2770–2780

Banerjee T, Murari V, Kumar M, Raju MP (2015) Source apportionment of airborne particulates through receptor modelling: Indian scenario. Atmos Res 164:167–187

Bangar V, Mishra AK, Jangid M, Rajput P (2021) Elemental characteristics and source apportionment of $PM_{2.5}$ during the post-monsoon season in Delhi India. Front Sustain Cities 3:648551

Banoo R, Gupta S, Gadi R et al (2024) Chemical characteristics, morphology and source apportionment of PM_{10} over National Capital Region (NCR) of India. Environ Monit Assess 196:163

Banoo R, Sharma SK, Gadi R, Gupta S, Mandal TK (2020) Seasonal variation of carbonaceous species of PM_{10} over urban sites of National Capital Region of India. Aerosol Sci Eng 4(2):11–123

Behera SN, Sharma M, Dikshit O et al (2011) GIS-Based emission inventory, dispersion modeling, and assessment for source contributions of particulate matter in an urban environment. Water Air Soil Pollut 218:423–436

Belis CA, Karagulian F, Larsen BR, Hopke PK (2013) Critical review and meta-analysis of ambient particulate matter source apportionment using receptor models in Europe. Atmos Environ 69:94–108

Bhuvaneshwari S, Hettiarachchi H, Meegoda JN (2019) Crop residue burning in India: policy challenges and potential solutions. Int J Environ Res Public Health 16:832

Brown SG, Eberly S, Paatero P, Norris GA (2015) Methods for estimating uncertainty in PMF solutions: examples with ambient air and water quality data and guidance on reporting PMF results. Sci Tot Environ 518–519:626–635

Bukowiecki N, Lienemann P, Hill M, Furger M, Richard A, Amato F, Prevot ASH, Baltensperger U, Buchmann B, Gehrig R (2010) PM_{10} emission factors for non-exhaust particles generated by road traffic in an urban street canyon and along a freeway in Switzerland. Atmos Environ 44:2330–2340

Chang Y, Huang K, Xie M, Deng C, Zou Z, Liu S, Zhang Y (2018) First long-term and near real-time measurement of trace elements in China's urban atmosphere: temporal variability, source apportionment and precipitation effect. Atmos Chem Phys 18:11793–11812

Chakraborty A, Gupta T (2010) Chemical characterization and source apportionment of submicron (PM_1) aerosol in Kanpur region, India. Aerosol Air Qual Res 10:433–445

Chelani A, Gajghate D, Chalapati Rao C, Devotta S (2010) Particle size distribution in ambient air of Delhi and its statistical analysis. Bull Environ Contam Toxicol 85:22–27

Chen P, Wang T, Kasoar M, Xie M, Li S, Zhuang B, Li M (2018) Source apportionment of $PM_{2.5}$ during haze and non-haze episodes in Wuxi China. Atmosphere 9:267

Chen CR, Lai HC, Liao MI, Hsiao MC, Ma HW (2021) Health risk assessment of trace elements of ambient $PM_{2.5}$ under monsoon patterns. Chemosphere 264:128462

Chen Y, Wild O, Ryan E, Sahu SK, Lowe D, Archer-Nicholls S, Wang Y, McFiggans G, Ansari T, Singh V, Sokhi RS, Archibald A, Beig G (2020) Mitigation of $PM_{2.5}$ and ozone pollution in Delhi: a sensitivity study during the pre-monsoon period. Atmos Chem Phys 20:499–514

Choudhary N, Srivastava P, Dutta M, Mukherjee S, Rai A, Kuniyal JC, Lata R, Chatterjee A, Naja M, Vijayan N, Mandal TK, Sharma SK (2022) Seasonal characteristics, sources and pollution pathways of PM_{10} at high altitudes himalayas of India. Aerosol Air Qual Res 22:7

Choudhary N, Rai A, Kuniyal JC, Srivastava P, Lata R, Dutta M, Ghosh A, Dey S, Sarkar S, Gupta S, Chaudhary S, Thakur I, Bawari A, Naja M, Vijayan N, Chatterjee A, Mandal TK, Sharma SK, Kotnala RK (2023) Chemical characterization and source apportionment of PM_{10} using receptor models over the Himalayan region of India. Atmosphere 14:880

Colonna KJ, Kotrakis P, Kinney PL, Cooke RM, Evans JS (2022) Mortality attributable to long-term exposure to ambient fine particulate matter: insight from the epidemiologic evidence for understudied locations. Environ Sci Technol 56:6799–6812

Crilley LR, Lucarelli F, Bloss WJ, Harrison RM, Beddows DC, Calzolai G, Nava S, Valli G, Bernardoni V, Vecchi R (2016) Source apportionment of fine and coarse particles at a roadside and urban background site in London during the 2012 summer Clear fLo campaign. Environ Pollut 220:766–778

Dai Q, Liu B, Bi X, Wu J, Liang D, Zhang Y, Feng Y, Hopke PK (2020) Dispersion normalized PMF provides insights into the significant changes in source contributions to $PM_{2.5}$ after the COVID-19 outbreak. Environ Sci Technol 54(16):9917–9927

Dockery DW, Pope CA, Xu X, Spengler JD, Ware JH, Fay ME, Ferris BG Jr, Speizer FE (1993) An association between air pollution and mortality in six US cities. New England J Medicine 329(24):1753–1759

Duan X, Yan Y, Li R, Deng M, Hu D, Peng L (2021) Seasonal variations, source apportionment, and health risk assessment of trace metals in $PM_{2.5}$ in the typical industrial city of Changsha. China Atmos Pollut Res 12:365–374

Fullova D, Durcanska D, Hegrova J (2017) Particulate matter mass concentrations produced from pavement surface abrasion. MATEC Web Conf 117:00048

Gianini MFD, Gehrig R, Fischer A, Ulrich A, Wichser A, Hueglin C (2012) Chemical composition of PM_{10} in Switzerland: an analysis for 2008/2009 and changes since 1998/1999. Atmos Environ 54:97–106

Grigoratos T, Martini G (2015) Brake wear particle emissions: a review. Environ Sci Pollut Res 22:2491–2504

Gugamsetty B, Wei H, Liu CN, Awasthi A, Hsu SC, Tsai CJ, Roam GD, Wu YC, Chen CF (2012) Source characterization and apportionment of PM_{10}, $PM_{2.5}$ and $PM_{0.1}$ by using positive matrix factorization. Aerosol Air Qual Res 12:476–491

Gupta I, Salunkhe A, Kumar R (2012) Source apportionment of PM_{10} by positive matrix factorization in urban area of Mumbai. The Scientific World Journal, India, p 585791

Gupta S, Sharma SK, Mandal TK (2023) Elemental analysis and health risk assessment of PM25 at an urban site of Delhi. In: Sanjay Y, Naveen G, Shankar GA, Shiv KJ, Harish K, Venu GA (eds) Recent Advances in Metrology. Springer, Berlin, pp 90–109

Harmens H, Norris DA, Steinnes E, Kubin E, Piispanen J, Alber R, Aleksiayenak Y, Blum O, Coskun M, Dam M (2010) Mosses as biomonitors of atmospheric heavy metal deposition: spatial patterns and temporal trends in Europe. Environ Pollut 158:3144–3156

IPCC (2013) Climate change 2013: The physical science basis. Contribution of working group I to the fifth assessment report of the intergovernmental panel on climate change In: Stocker TF, Qin D, Plattner GK, Tignor M, Allen SK, Boschung J, Nauels A, Xia Y, Bex V, Midgley PM (eds.), Cambridge University Press: Cambridge, pp 1535

Jain S, Sharma SK, Choudhary N, Masiwal R, Saxena M, Sharma A, Mandal TK, Gupta A, Gupta NC, Sharma C (2017) Chemical characteristics and source apportionment of $PM_{2.5}$ using PCA/APCS, UNMIX and PMF at an urban site of Delhi. India Environ Sci Pollut Res 24:14637–14656

Jain S, Sharma SK, Mandal TK, Saxena M (2018) Source apportionment of PM_{10} using PCA/APCS, in Delhi, India using PCA/APCS, UNMIX and PMF. Particuology 37:107–118

Jain S, Sharma SK, Srivastava MK, Chatterjee A, Singh RK, Saxena M, Mandal TK (2019) Source apportionment of PM_{10} over three tropical urban atmospheres at Indo-Gangetic Plain of India: an approach using different receptor models. Arch Environ Contam Toxicol 76(1):114–128

Jain S, Sharma SK, Vijayan N, Mandal TK, Saxena M (2020) Seasonal characteristics of aerosols ($PM_{2.5}$ and PM_{10}) and their source apportionment using PMF: a four-year study over Delhi India. Environ Pollut 262:114337

Jain S, Sharma SK, Vijayan N, Mandal TK (2020) Investigating the seasonal variability in source contribution to PM models during 2013–2016 in Delhi, India. Environ Sci Pollut Res 28:1–16

Jain S, Sharma SK, Srivastava MK, Chatterjee A, Vijayan N et al (2021) Chemical characterization, source apportionment and transport pathways of $PM_{2.5}$ and PM_{10} over Indo-Gangetic Plain of India. Urban Clim 36:100805

Jeong JH, Shon ZH, Kang M, Song SK, Kim YK, Park J, Kim H (2017) Comparison of source apportionment of $PM_{2.5}$ using receptor models in the main hub port city of East Asia: Busan. Atmos Environ 148:115–127

Jerret M (2015) Atmospheric science: the death toll from air-pollution sources. Nature 525:330–331

Jiang N, Li Q, Su F, Wang Q, Yu X, Kang P, Zhang R, Tang X (2018) Chemical characteristics and source apportionment of $PM_{2.5}$ between heavily polluted days and other days in Zhengzhou. China J Environ Sci 66:188–198

Jin L, Apte JS, Miller SL, Tao S, Wang S, Jiang G, Li X (2022) Global endeavors to address the health effects of urban air pollution. Environ Sci Technol 56:6793–6798

Joshi P, Dey S, Ghosh S, Jain S, Sharma SK (2022) Association between acute exposure to $PM_{2.5}$ chemical species and mortality in megacity Delhi India. Environ Sci Technol 56:7275–7287

Karar K, Gupta AK (2007) Source apportionment of PM_{10} at residential and industrial sites of an urban region of Kolkata India. Atmos Res 84:30–41

Kelly FJ, Fussell JC (2012) Size, source and chemical composition as determinants of toxicity attributable to ambient particulate matter. Atmos Environ 60:504–526

Khan MF, Latif MT, Saw WH, Amil N, Nadzir MSM, Sahani M, Tahir NM, Chung JX (2016) Fine particulate matter in the tropical environment: monsoonal effects, source apportionment, and health risk assessment. Atmos Chem Phys 16:597–617

Lelieveld J, Evans JS, Fnais M, Giannadaki D, Pozzer A (2015) The contribution of outdoor air pollution sources to premature mortality on a global scale. Nature 525:367–371

Li Y, Liu B, Xue Z, Zhang Y, Sun X, Song C et al (2020) Chemical characteristics and source apportionment of $PM_{2.5}$ using PMF modelling coupled with 1-hr resolution online air pollutant dataset for Linfen China. Environ Poll 263(B):114532

Li R, Gao Y, Chen Y, Peng M, Zhao W, Wang G, Hao J (2023) Measurement report: rapid changes of chemical characteristics and health risks for highly time resolved trace elements in $PM_{2.5}$ in a typical industrial city in response to stringent clean air actions. Atmos Chem Phys 23:4709–4726

Liao HT, Lee CL, Tsai WC, Yu JH, Tsai SW et al (2021) Source apportionment of urban $PM_{2.5}$ using positive matrix factorization with vertically distributed measurements of trace elements and nonpolar organic compounds. Atmos Poll Res 12(4):200–207

Leri AC, Heltithanthri O, Bolan S, Zheng T et al (2024) Bromine contamination and risk management in terrestrial and aquatic ecosystems. J Hazard Mater 469:133881

Lopez-Cruz J, Crespo-Salvador O, Fernandez-Crespo E, Garcia-Agustin P, Gonzalez-Bosch C (2016) Absence of Cu Zn superoxide dismutase BCSOD1 reduces botrytis cinerea virulence in arabidopsis and tomato plants, revealing interplay among reactive oxygen species, callose and signaling pathways. Mol Plant Pathol 18:16–31

Ma W, Tai L, Qiao Z, Zhong L, Wang Z, Fu K et al (2018) Contamination source apportionment and health risk assessment of heavy metals in soil around municipal solid waste incinerator: a case study in North China. Sci Total Environ 631–632:348–357

Maenhaut W (2017) Source apportionment revisited for long-term measurements of fine aerosol trace elements at two locations in southern Norway. Nucl Instrum Meth B 417:133–138

Manousakas M, Furger M, Daellenbach KR, Canonaco F, Chen G, Tobler A, Rai P et al (2022) Source identification of the elemental fraction of particulate matter using size segregated, highly time-resolved data and an optimized source apportionment approach. Atmos Environ-X 14:100165

Meng Y, Li R, Cui L, Wang Z, Fu H (2022) Phosphorus emission from open burning of major crop residues in China. Chemosphere 288:132568

Micheline G, Rachida C, Celine M, Gaby K, Rachid A, Petru J (2019) Levels of Pb, Cd, Hg and As in fishery products from the eastern Mediterranean and human health risk assessment due to their consumption. Intern J Environ Res 13:443–455

Murari V, Singh N, Ranjan R, Singh RS, Banerjee T (2020) Source apportionment and health risk assessment of airborne particulates over central Indo-Gangetic plain. Chemosphere 257:127145

Naja M, Mallik C, Sarangi T, Sheel V, Lal S (2014) SO_2 measurements at a high-altitude site in the central himalayas: role of regional transport. Atmos Environ 99:392–402

Oldani KM, Mladenov N, Williams M, Campbell CM, Lipson DA (2017) Seasonal patterns of dry deposition at a high elevation site in the Colorado Rocky Mountains. J Geophys Res-Atmos 122:11183–11200

Paatero P (1997) Least squares formulation of robust non-negative factor analysis. Chem Intell Lab Syst 37(1):23–35

Paatero P, Tapper U (1994) Positive matrix factorization: a non-negative factor model with optimal utilization of error estimates of data values. Environmetrics 5(2):111–126

Peng X, Wang W, Xia M, Cheng H et al (2021) An unexpected large continental source of reactive bromine and chlorine with significant impact on wintertime air quality. Natl Sci Rev 8(7):nwaa304

Pope CA, Ezzati M, Dockery DW (2009) Fine-particulate air pollution and life expectancy in the United States. New Engl J Med 360:376–386

Prakash J, Lohia T, Mandariya AK, Habib G, Gupta T, Gupta SK (2018) Chemical characterization and quantitative assessment of source-specific health risk of trace metals in $PM_{1.0}$ at a road site of Delhi. India Environ Sci Pollut Res 25:8747–8764

Rai A, Mukherjee S, Chatterjee A, Choudhary N, Kotnala G, Mandal TK, Sharma SK (2020a) Seasonal variation of OC, EC, and WSOC of PM_{10} and their CWT analysis over the eastern Himalaya. Aerosol Sci Eng 4:26–40

Rai P, Furger M, El Haddad I, Kumar V, Wang L, Singh A, Dixit K, Bhattu D, Petit JE, Ganguly D, Rastogi N (2020b) Real-time measurement and source apportionment of elements in Delhi's atmosphere. Sci Total Environ 742:140332

Rai P, Slowik JG, Furger M, El Haddad I, Visser S (2021) Highly time-resolved measurements of element concentrations in PM_{10} and $PM_{2.5}$: comparison of Delhi, Beijing, London, and Karakow. Atmos Chem Phys 21:717–730

Ram K, Sarin MM, Tripathi SN (2010) One-year record of carbonaceous aerosols from an urban location (Kanpur) in the Indo-Gangetic plain: characterization, sources and temporal variability. J Geophys Res 115:D24313

Saffari A, Daher N, Shafer MM, Schauer JJ, Sioutas C (2014) Global perspective on the oxidative potential of airborne particulate matter: a synthesis of research findings. Environ Sci Technol 48:7576–7583

Saraswati SSK, Saxena M, Mandal TK (2019) Characteristics of gaseous and particulate ammonia and their role in the formation of secondary inorganic particulate matter at Delhi, India. Atmos Res 218:34–49

Sah D, Verma PK, Kumari KM, Lakhani A (2022) Characterisation, sources and health risk of heavy metals in $PM_{2.5}$ in Agra India. Exposure and Health 49:10147

Sharma SK, Choudhary N, Kotnala G, Das D, Mukherjee S, Ghosh A, Vijayan N, Rai A, Chatterjee A, Mandal TK (2020) Wintertime carbonaceous species and trace metals in PM_{10} in Darjeeling: a high-altitude town in the eastern Himalayas. Urban Clim 34:100668

Sharma SK, Mandal TK (2023) Elemental composition and sources of fine particulate matter ($PM_{2.5}$) in Delhi India. Bull Environ Contam Toxicol 110:60

Sharma SK, Mandal TK, Saxena M, Sharma A, Gautam R (2014) Source apportionment of PM_{10} by using positive matrix factorization at an urban site of Delhi, India. Urban Clim 10:656–670

Sharma SK, Mandal TK, Jain S et al (2016a) Source apportionment of $PM_{2.5}$ in Delhi, India using PMF model. Bull Environ Contam Toxicol 97:286–293

Sharma SK, Mandal TK, Srivastava MK et al (2016b) Spatio-temporal variation in chemical characteristics of PM_{10} over Indo Gangetic plain of India. Environ Sci Pollut Res 23:18809–18822

Sharma SK, Mandal TK (2017) Chemical composition of fine mode particulate matter ($PM_{2.5}$) at an urban area of Delhi and its source apportionment. Urban Clim 21:106–122

Sharma SK, Mandal TK, Banoo R, Rai A, Rani M (2022) Long-term variation in carbonaceous components of $PM_{2.5}$ from 2012–2021 in Delhi. Bull Environ Contamin Toxicol 109:502–510

Sharma SK, Mukherjee S, Choudhary N, Rai A, Ghosh A, Chatterjee A, Vijayan N, Mandal TK (2021) Seasonal variation and sources of carbonaceous species and elements in $PM_{2.5}$ and PM_{10} over the eastern Himalaya. Environ Sci Pollut Res 28:51642–51656

Shivani GR, Sharma SK, Mandal TK (2019) Seasonal variation, source apportionment and source attributed health risk of fine carbonaceous aerosols over National Capital Region. India Chemosphere 237:124500

Singh RK (2019) Assessment of ambient air pollution and mitigation strategies towards achieving air quality index (AQI) in the Indian Himalayan Region. Int J Sci Res 9:12

Singh N, Singh A, Banerjee T, Chakarborty A, Deboudt K, Mohan M (2023) source specific health risks of size segregated particulate bound metals in an urban environment over northern India. Atmos Environ 314:120091

Singhal A, Habib G, Raman RS, Gupta T (2017) Chemical characterization of $PM_{1.0}$ aerosol in Delhi and source apportionment using positive matrix factorization. Environ Sci Poll Res 24:445–462

Srimuruganandam B, Shiva Nagendra SM (2012) Application of positive matrix factorization in characterization of PM_{10} and $PM_{2.5}$ emission sources at urban roadside. Chemosphere 88(1):120–30

Storelli MM (2008) Potential human health risks from metals (Hg, Cd, and Pb) and polychlorinated biphenyls (PCBs) via seafood consumption: estimation of target hazard quotients (THQs) and toxic equivalents (TEQs). Food Chem Toxicol 46:2782–2788

Uria-Tellaetxe I, Carslaw DC (2014) Conditional bivariate probability function for source identification. Environ Model Softw 59:1–9

US EPA (2011) Exposure Factors Handbook 2011 Edition (Final Report). U.S. Environmental Protection Agency, Washington, DC (EPA/600/R-09/052F)

Verma A, Ranga V, Vishwakarma DK (2023) A novel approach for forecasting PM25 pollutions in Delhi using CATALYST. Environ Monit Assess 195(12):1457

Waked A, Favez O, Alleman LY, Piot C, Petit JE, Delaunay T, Verlinden E, Golly B, Besombes JL, Jaffrezo JL, Leoz-Garziandia E (2014) Source apportionment of PM_{10} in a north-western Europe regional urban background site (Lens, France) using positive matrix factorization and including primary biogenic emissions. Atmos Chem Phys 14:3325–3346

Wang W, Chen C, Liu D, Wang M, Han Q, Zhang X, Feng X, Sun A, Mao P, Xiong Q, Zhang C (2022) Health risk assessment of $PM_{2.5}$ heavy metals in county units of northern China based on Monte Carlo simulation and APCS-MLR. Sci Total Environ 843: 156777.

Watson JG, Chow JC, Frazier CA (1999) X-ray fluorescence analysis of ambient air samples. In: Elemental Analysis of Airborne Particles. Gordon and Breach Science: Amsterdam, vol 1, pp 67–96

WHO (2016) WHO global urban ambient air pollution database by world health organization. Department of public health. Environmental and social determinants of health. World health organisation, 1211 Geneva 27, Switzerland.

World Health Organization (2016) Ambient air pollution: A global assessment of exposure and burden of disease. Department of public health. Environmental and social determinants of health. World health organisation, 1211 Geneva 27, Switzerland.

Zhang N, Maung MW, Win MS, Feng J, Yao X (2022) Carbonaceous aerosol and inorganic ions of $PM_{2.5}$ in Yangon and Mandalay of Myanmar: seasonal and spatial variations in composition and sources. Atmos Pollut Res 13(6):101444

Zhang J, Zhou X, Wang Z, Yang L, Wang J, Wang W (2018) Trace elements in $PM_{2.5}$ in Shandong Province: source identification and health risk assessment. Sci Total Environ 621:558–577

Zheng N, Liu J, Wang Q, Liang Z (2010) Health risk assessment of heavy metal exposure to street dust in the zinc smelting district. Northeast China Sci Total Environ 408(4):726–733

Zhu C, Tian H, Hao J (2020) Global anthropogenic atmospheric emission inventory of twelve typical hazardous trace elements, 1995–2012. Atmos Environ 220:117061